13 Pillar supported mining methods

13.1 Components of a supported mine structure

A mining method based on pillar support is intended to control rock mass displacements throughout the zone of influence of mining, while mining proceeds. This implies maintenance of the local stability of rock around individual excavations and more general control of displacements in the mine near-field domain. As a first approximation, stope local stability and near-field ground control might be considered as separate design issues, as indicated schematically in Figure 13.1. Stopes may be excavated to be locally self-supporting, if the principles described in Chapters 7–9 are applied in their design. Near-field ground control is achieved by the development of load-bearing elements, or pillars, between the production excavations. Effective performance of a pillar support system can be expected to be related to both the dimensions of the individual pillars and their geometric location in the orebody. These factors are related intuitively to the load capacity of pillars and the loads imposed on them by the interacting rock mass.

Leaving pillar support in an orebody results in either temporary or permanent sterilisation of a fully proven and developed mining reserve. An economic design of a support system implies that ore committed to pillar support be a minimum, while fulfilling the essential requirement of assuring the global stability of the mine structure. Therefore, detailed understanding of the properties and performance of pillars and pillar systems is essential in mining practice, to achieve the maximum, safe economic potential of an orebody.

Room-and-pillar mining, and the several versions of longhole, open and bench stoping, represent the main methods based on temporary or permanent pillar support.

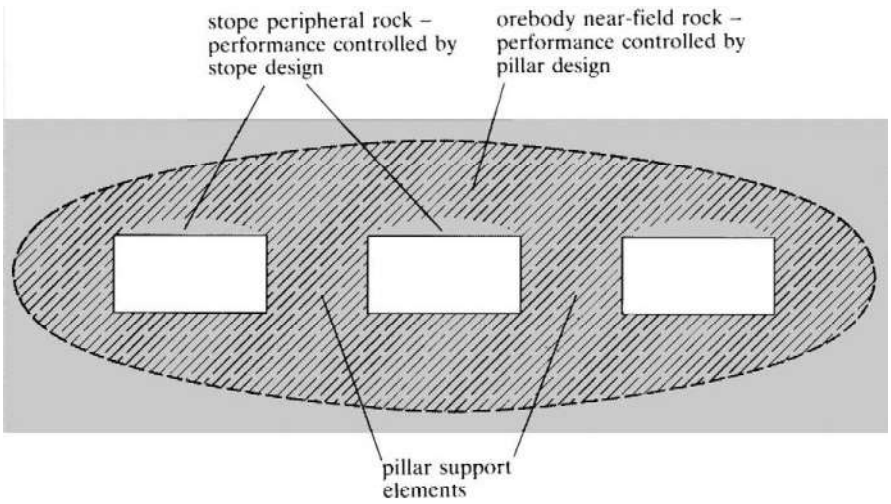

Figure 13.1 Schematic illustration of problems of mine near-field stability and stope local stability, affected by different aspects of mine design.

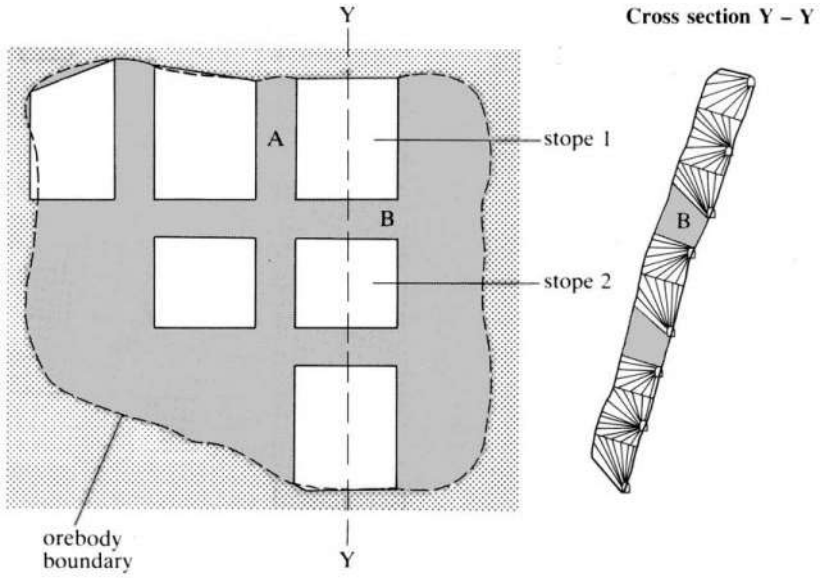

Figure 13.2 Pillar layout for extraction of an inclined orebody, showing biaxially confined transverse and longitudinal pillars, 'A' and 'B', respectively.

In these various methods, clear differences exist between the ways in which pillars are generated and the states of loading and confinement applied to individual pillars. For example, pillars in flat-lying, stratiform orebodies are frequently isolated on four sides, providing a resistance to imposed displacement that is essentially uniaxial. Interaction between the pillar ends and the country rock results in heterogeneous, triaxial states of stress in the body of the pillar, even though it is uniaxially loaded by the abutting rock. A set of uniaxially loaded pillars is illustrated in Figure 12.2. An alternative situation is shown in Figure 13.2. In this case, the pillars generated by open stoping are biaxially loaded by the country rock.

The terminology used in denoting the support mode of a pillar reflects the principal direction of the resistance imposed by it to displacement of the country rock. Each of the pillars illustrated in Figure 12.2 is a vertical pillar. For a biaxially loaded or confined pillar, the direction corresponding to the smaller dimension of loading is used to denote its primary mode of support. The pillar labelled 'A' in Figure 13.2 is a horizontal, transverse pillar, while the pillar labelled 'B' is a horizontal, longitudinal pillar. Pillar 'B' could also be called the floor pillar for stope '1', or the crown pillar for stope '2'. If the longitudinal pillar persisted along the strike of the orebody for several stope and pillar blocks, it might be called a chain pillar.

In the mine structures illustrated in Figures 12.2 and 13.2, failure of pillars to sustain the imposed states of stress may result in extensive collapse of the adjacent near-field rock. If the volume of the unfilled mined void is high, the risk is that collapse may propagate through the pillar structure. In an orebody that is extensive in two dimensions, this possibility may be precluded by dividing the deposit into mine districts, or panels, separated by barrier pillars. A plan view of such a schematic layout is shown in Figure 13.3. The barrier pillars are designed to be virtually indestructible, so that each panel performs as an isolated mining domain. The maximum extent of any collapse is then restricted to that of any mining panel. Obviously, the principles applied in the design of panel pillars will be different from those for barrier pillar design, due

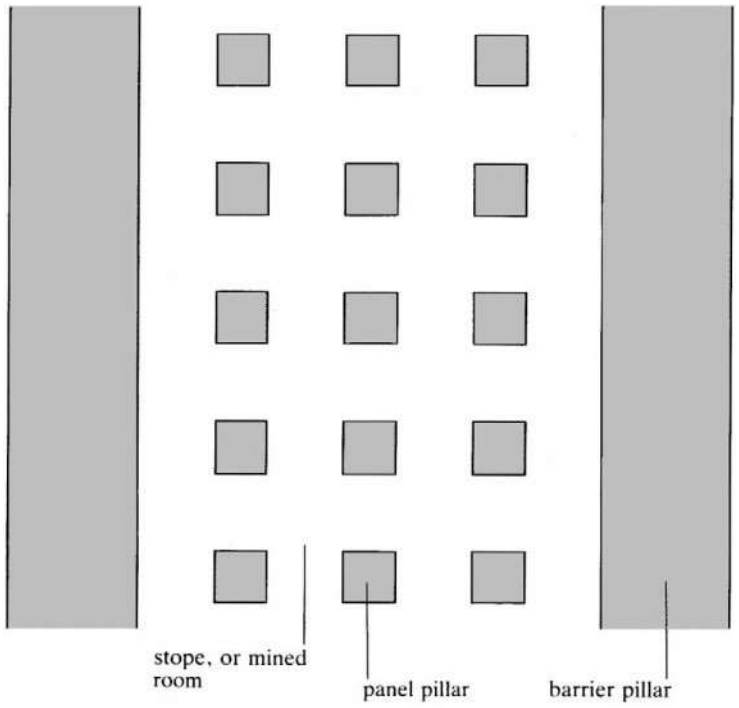

Figure 13.3 Layout of barrier pillars and panel pillars in a laterally extensive orebody.

to their different functions. In the following discussion, attention is confined to the performance and design of panel pillars, since their rôle is that most frequently and generally exploited in stoping practice.

13.2 Field observations of pillar performance

The most convenient observations of pillar response to induced mining loads and displacements are made in room and pillar operations, since the method allows direct access to the pillar sites. Detailed observation and measurement of pillar behaviour have been reported by many researchers, including Bunting (1911), Greenwald *et al.* (1939, 1941), Hedley and Grant (1972), Wagner (1974, 1980), Van Heerden (1975), Hardy and Agapito (1977), and Hedley *et al.* (1984). Some particularly useful summaries on pillar performance, analysis of their load-bearing capacity and pillar design have been provided by Salamon and Munro (1967), Coates (1981) and Lunder and Pakalnis (1997). For purposes of illustration, the initial discussion which follows is concerned with pillars subject to nominal uniaxial loading. Subsequent discussion takes account of more complex states of stress in pillars.

Stoping activity in an orebody causes stress redistribution and an increase in pillar loading, illustrated conceptually in Figure 13.4. For states of stress in a pillar less than the *in situ* rock mass strength, the pillar remains intact and responds elastically to the increased state of stress. Mining interest is usually concentrated on the peak load-bearing capacity of a pillar. Subsequent interest may then focus on the post-peak, or ultimate load-displacement behaviour, of the pillar.

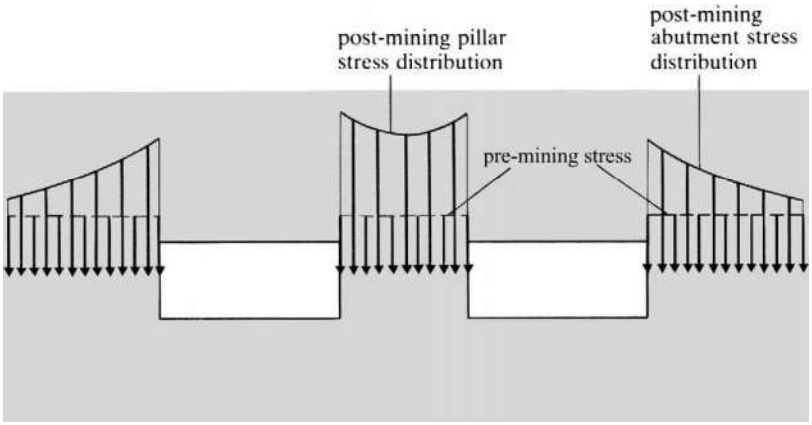

Figure 13.4 Redistribution of stress in the axial direction of a pillar accompanying stope development.

The structural response of a pillar to mining-induced load is determined by the rock material properties, the geological structure, the absolute and relative dimensions of the pillar and the nature of surface constraints applied to the pillar by the country rock. Three main modes of pillar behaviour under stresses approaching the rock mass strength have been recognised, which may be reproduced qualitatively by laboratory tests on model pillars in a displacement controlled testing machine. These failure modes are illustrated in Figure 13.5.

In relatively massive rock, the most obvious sign of pillar stressing involves spalling from the pillar surfaces, as illustrated in Figure 13.5a. Fretting or necking of the pillar occurs. In a detailed study, Lunder and Pakalnis (1997) described the progressive stages of degradation of a pillar in terms of the modes of deformation represented in Figure 13.6. Although the initial signs of rock stress may be local shear failure, associated with the re-entrant geometry represented in Figure 13.6a, the formation of surface spalls illustrated in Figure 13.6b is a more extensive failure indicative of states of stress satisfying the conditions for fracture initiation and rock damage in a significant volume of the pillar. In this condition, the pillar is partially failed, but the core of the pillar is intact, in terms of the model of rock fracture and failure discussed in Chapter 4. Higher states of stress lead to damage accumulation through internal crack initiation and extension, and interaction of the network of cracks, as shown in Figure 13.6c. When friction between the fully developed crack population is fully mobilized, the pillar is at peak strength, and mechanically is at a state of failure, illustrated in Figure 13.6d. This model of the progressive evolution of pillar failure is consistent with the micromechanical modelling of pillar loading reported by Diederichs (2002), in which progressive crack formation and localisation of shear strain was observed.

The effect of pillar relative dimensions on failure mode is illustrated in Figure 13.5b. For regularly jointed orebody rock, a high pillar height/width ratio may favour the formation of inclined shear fractures transecting the pillar. There are clearly kinematic factors promoting the development of penetrative, localised shear zones of this type. Their occurrence has been reproduced in model tests by Brown (1970), under the geometric conditions prescribed above.

The third major mode of pillar response is expressed in an orebody with highly deformable planes of weakness forming the interfaces between the pillar and the

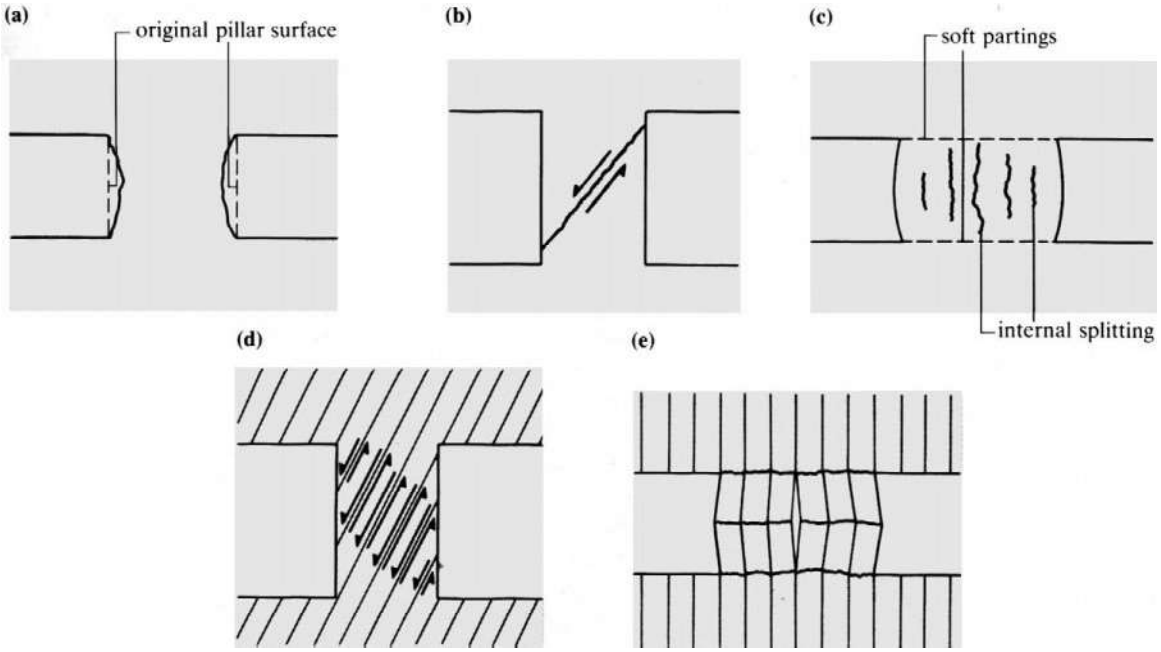

Figure 13.5 Principal modes of deformation behaviour of mine pillars.

adjacent country rock. Yield of the soft layers generates transverse tractions over the pillar end surfaces and promotes internal axial splitting of the pillar. This may be observed physically as lateral bulging or barrelling of the pillar surfaces. Geomechanical conditions favouring this mode of response may occur in stratiform orebodies, where soft bedding plane partings define the foot wall and hanging wall for the orebody. The failure condition is illustrated in Figure 13.5c.

Other specific modes of pillar response may be related directly to the structural geology of the pillar. For example, a pillar with a set of natural transgressive fractures, as illustrated in Figure 13.5d, can be expected to yield if the angle of inclination of the fractures to the pillar principal plane (that perpendicular to the pillar axis) exceeds their effective angle of friction. The amount of slip on the fractures required for yield,

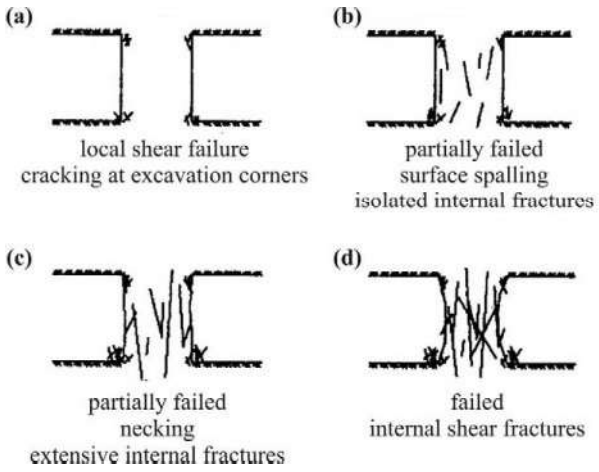

Figure 13.6 Schematic illustration of the evolution of fracture and failure in a pillar in massive rock (after Lunder and Pakalnis, 1997).

and subsequent relaxation of the elastic state of stress in the pillar, need only be of elastic orders of magnitude. A pillar (or other rock remnant in a mine layout) with a well-developed foliation or schistosity parallel to the principal axis of loading will fail in a buckling mode, as illustrated in Figure 13.5e. This mechanism resembles the formation of kink bands.

Field observations of pillars subject to biaxial loading are usually difficult, due to the mine geometries in which they occur. However, observations reported by Brady (1977), Krauland and Soder (1987), Sjöberg (1992) and Diederichs *et al.* (2002) suggest that the modes of response for biaxially loaded pillars are consistent with those for uniaxial loading. A similar conclusion is implied in the work by Wagner (1974).

13.3 Elementary analysis of pillar support

In the analysis and prediction of the behaviour of a set of pillars in a mine structure, the computational techniques described in Chapter 6 could be used for detailed determination of the state of stress throughout the rock mass. However, some instructive insights into the properties of a pillar system can be obtained from a much simpler analysis, based on elementary notions of static equilibrium. These are used to establish an average state of stress in the pillars, which can then be compared with an average strength of the rock mass representative of the particular pillar geometry. Notwithstanding the limitations of this approach, Lunder and Pakalnis (1997) proposed that it is possible to reconcile the analysis of pillar stress using the tributary area method with more rigorous analysis using computational methods.

Figure 13.7a shows a cross section through a flat-lying orebody, of uniform thickness, being mined using long rooms and rib pillars. Room spans and pillar spans are w_o and w_p respectively. For a sufficiently extensive set of rooms and pillars, a representative segment of the mine structure is as shown in Figure 13.7b. Considering the requirement for equilibrium of any component of the structure under the internal forces and unit thickness in the antiplane direction, the free body shown in

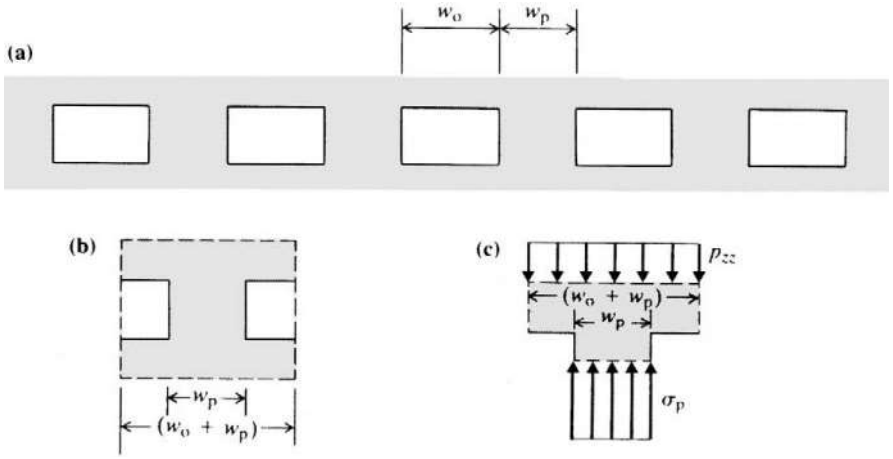

Figure 13.7 Bases of the tributary area method for estimating average axial pillar stress in an extensive mine structure, exploiting long rooms and rib pillars.

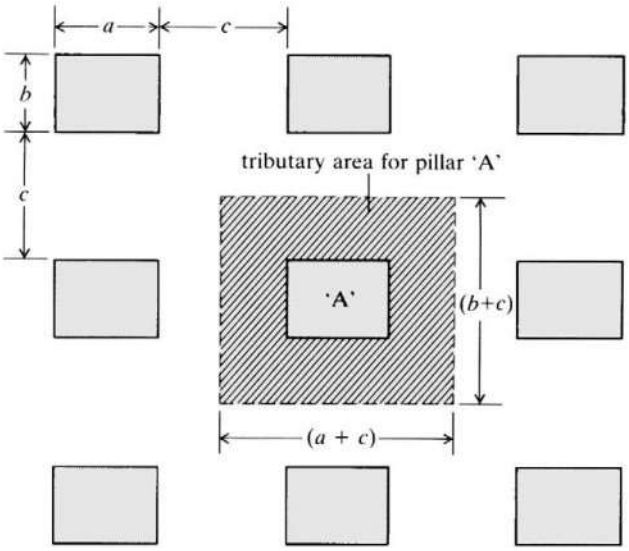

Figure 13.8 Geometry for tributary area analysis of pillars in uniaxial loading.

Figure 13.7c yields the equation

$$\sigma_p w_p = p_{zz}(w_o + w_p)$$

or

$$\sigma_p = p_{zz}(w_o + w_p)/w_p \tag{13.1}$$

In this expression, σ_p is the average axial pillar stress, and p_{zz} is the vertical normal component of the pre-mining stress field. The width $(w_o + w_p)$ of the representative free body of the pillar structure is often described as the area which is tributary to the representative pillar. The term 'tributary area method' is therefore used to describe this procedure for estimating the average state of axial stress in the pillar. A quantity of practical interest in mining an orebody of uniform thickness is the area extraction ratio, r, defined by (area mined)/(total area of orebody). Considering the representative element of the orebody illustrated in Figure 13.7c, the area extraction ratio is also defined by

$$r = w_o/(w_o + w_p)$$

so that

$$1 - r = w_p/(w_o + w_p)$$

Insertion of this expression in equation 13.1 yields

$$\sigma_p = p_{zz}[1/(1 - r)] \tag{13.2}$$

The mining layout shown in plan in Figure 13.8, involving pillars of plan dimensions a and b, and rooms of span c, may be treated in an analogous way. The area tributary

to a representative pillar is of plan dimensions $(a + c)$, $(b + c)$, so that satisfaction of the equation for static equilibrium in the vertical direction requires

$$\sigma_p \, ab = p_{zz}(a + c)(b + c)$$

or

$$\sigma_p = p_{zz}(a + c)(b + c)/ab \tag{13.3}$$

The area extraction ratio is defined by

$$r = [(a + c)(b + c) - ab]/(a + c)(b + c)$$

and some simple manipulation of equation 13.3 produces the expression

$$\sigma_p = p_{zz}[1/(1 - r)]$$

which is identical with equation 13.2.

For the case where square pillars, of plan dimension $w_p \times w_p$, are separated by rooms of dimension w_o, equation 13.3 becomes

$$\sigma_p = p_{zz}[(w_o + w_p)/w_p]^2 \tag{13.4}$$

Of course, average axial pillar stress is still related to area extraction ratio through equation 13.2.

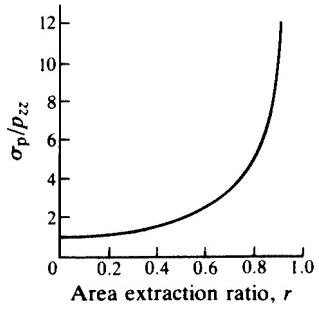

Figure 13.9 Variation of pillar stress concentration factor with area extraction ratio.

Equations 13.1, 13.3, and 13.4 suggest that the average state of axial stress in a representative pillar of a prospective mining layout can be calculated directly from the stope and pillar dimensions and the pre-mining normal stress component acting parallel to the pillar axis. It is also observed that for any geometrically uniform mining layout, the average axial pillar stress is directly determined by the area extraction ratio. The relation between pillar stress level and area extraction ratio is illustrated graphically in Figure 13.9. The principal observation from the plot is the high incremental change in pillar stress level, for small change in extraction ratio, when operating at high extraction ratio. For example, a change in r from 0.90 to 0.91 changes the pillar stress concentration factor from 10.00 to 11.11. This characteristic of the equation governing stress concentration in pillars clearly has significant design and operational implications. It explains why extraction ratios greater than about 0.75 are rare when natural pillar support is used exclusively in a supported method of working. Below this value of r, incremental changes in σ_p/p_{zz} with change in r are small. For values of r greater than 0.75, the opposite condition applies.

When calculating pillar axial stress using the tributary area method, it is appropriate to bear in mind the implicit limitations of the procedure. First, the average axial pillar stress is purely a convenient quantity for representing the state of loading of a pillar in a direction parallel to the principal direction of confinement. It is not simply or readily related to the state of stress in a pillar which could be determined by a complete analysis of stress. Second, the tributary area analysis restricts attention to the pre-mining normal stress component directed parallel to the principal axis of the pillar support system. The implicit assumption that the other components of the pre-mining

stress field have no effect on pillar performance is not generally tenable. Finally the effect of the location of a pillar within an orebody or mine panel is ignored.

The tributary area method provides a simple method of determining the average state of axial stress in a pillar. Prediction of the *in situ* performance of a pillar requires a method of assessing the strength or peak resistance of the pillar to axial compression. Retrospective analysis of the *in situ* performance of pillars, using the tributary area method to estimate imposed pillar stresses, suggests that the strength of a pillar is related to both its volume and its geometric shape. The effect of volume on strength can be readily understood in terms of a distribution of cracks, natural fractures and other defects in the rock mass. Increasing pillar volume ensures that the defect population is included representatively in the pillar. The shape effect arises from three possible sources: confinement which develops in the body of a pillar due to constraint on its lateral dilation, imposed by the abutting country rock; redistribution of field stress components other than the component parallel to the pillar axis, into the pillar domain; change in pillar failure mode with change in aspect (i.e. width/height) ratio. The second of these factors is, in fact, an expression of an inherent deficiency of the tributary area method.

The historical development of formulae for pillar strength is of considerable practical interest. As noted by Hardy and Agapito (1977), the effects of pillar volume and geometric shape on strength S are usually expressed by an empirical power relation of the form

$$S = S_o v^a (w_p / h)^b = S_o v^a R^b \tag{13.5}$$

In this expression, S_o is a strength parameter representative of both the orebody rock mass and its geomechanical setting, v, w_p and h are pillar volume, width and height respectively, R is the pillar width/height ratio, and a and b reflect geo-structural and geomechanical conditions in the orebody rock.

Examination of equation 13.5 might suggest that if strength tests were performed on a unit cube of orebody rock (i.e. 1 m^3, each side of length 1 m), the value of the representative strength parameter S_o could be measured directly. Such an interpretation is incorrect, since equation 13.5 is not dimensionally balanced. Acceptable sources of a value for S_o are retrospective analysis of a set of observed pillar failures, in the geomechanical setting of interest, or by carefully designed *in situ* loading tests on model pillars. The loading system described by Cook, N.G.W. *et al.* (1971), involving the insertion of a jack array in a slot at the midheight of a model pillar, appears to be most appropriate for these tests, since it preserves the natural boundary conditions on the pillar ends.

An alternative expression of size and shape effects on pillar strength is obtained by recasting equation 13.5 in the form

$$S = S_o h^\alpha w_p^\beta \tag{13.6}$$

For pillars which are square in plan, the exponents α, β, a, b in equations 13.5 and 13.6 are linearly related, through the expressions

$$a = \frac{1}{3}(\alpha + \beta), \quad b = \frac{1}{3}(\beta - 2\alpha)$$

Table 13.1 Exponents determining pillar strength from its volume and shape (equations 13.5 and 6) (from Salamon and Munro, 1967).

Source	α	β	a	b	Subject medium
Salamon and Munro (1967)	-0.66 ± 0.16	0.46	-0.067 ± 0.048	0.59 ± 0.14	South African coal; *in situ* failures
Greenwald *et al.* (1939)	−0.83	0.50	−0.111	0.72	Pittsburgh coal; model tests
Steart (1954); Holland and Gaddy (1957)	−1.00	0.50	−0.167	0.83	West Virginia coal; laboratory tests
Skinner (1959)	–	–	−0.079	–	hydrite; laboratory tests

Salamon and Munro (1967) summarise some estimated values of the pillar strength exponents for square pillars, determined from various sources. The values are presented in Table 13.1.

Equation 13.6 suggests pillar strength is a simple function of pillar width and height. However, a study reviewed by Wagner (1980) indicated that the operating area (defined by the pillar dimensions perpendicular to the pillar axis) is important. Measurement of the load distribution in a pillar at various states of loading, as shown in Figure 13.10, showed that failure commenced at the pillar boundary and migrated towards the centre. At the stage where structural failure of the pillar had occured, the core of the pillar had not reached its full load-bearing potential. Further, it was proposed that the relative dimensions of the pillar operating area had a substantial influence on pillar strength. This led to definition of the effective width, w_p^e, of a pillar of irregular shape, given by

$$w_p^e = 4A_p/C \tag{13.7}$$

where A_p is the pillar operating area and C is the pillar circumference.

In the application of this expression for pillar effective width, pillar strength may be estimated from equations 13.5 and 13.6, with w_p replaced by w_p^e. It is notable that equation 13.7 indicates that, for long rib pillars, with $l_p \gg w_p$, $w_p^e = 2w_p$. This is consistent with the field observation that rib pillars are significantly stronger than square pillars of the same width.

When equation 13.6 is applied to pillars with width-to-height ratio greater than about four or five, pillar strength is underestimated substantially. For these pillars with so-called squat aspect ratios, Wagner and Madden (1984) propose that equation 13.5 can be modified to incorporate terms which reflect more accurately the effect of aspect ratio on strength. The modified pillar strength expression has the form

$$S = S_o v^a R_o^b \{(b/\varepsilon)[(R/R_o)^\varepsilon - 1] + 1\}, \quad R > R_o \tag{13.8}$$

In this expression, ε is a parameter with magnitude $\varepsilon > 1$ which describes the rate of strength increase when aspect ratio R is greater than a nominal aspect ratio R_o at which equation 13.6 is no longer valid. Values suggested for R_o and ε which lead to conservative estimates of squat pillar strength are 5 and 2.5 respectively.

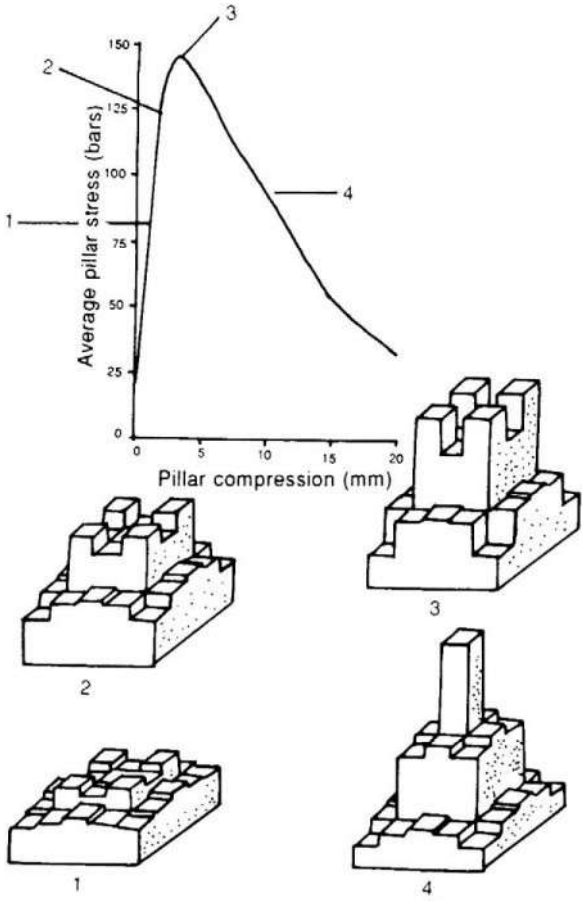

Figure 13.10 Distribution of vertical stress in a coal pillar at various stages of pillar failure (after Wagner, 1980).

Galvin *et al.* (1999) have further developed the approach outlined in the preceding paragraphs by adding more recent data for failed and unfailed pillars from Australian and South African coal mines and re-analysing the combined database. They also modified the previous analysis to establish a new minimum critical pillar width for pillars whose bases may be represented as parallelepipeds. With reference to Figure 13.11, Galvin *et al.* (1999) re-wrote equation 13.7 as

$$w_{eo} = \Theta_o w \tag{13.9}$$

where w is the minimum width of the pillar (i.e. $w = w_1 \sin\theta$) and the dimensionless parameter Θ_o is defined by

$$\Theta_o = 2w_2/(w_1 + w_2) \tag{13.10}$$

The range taken by this parameter is $1 \leq \Theta_o < 2$ as the plan aspect ratio of the pillar ranges from unity towards infinity. Galvin *et al.* (1999) suggest that the effective width

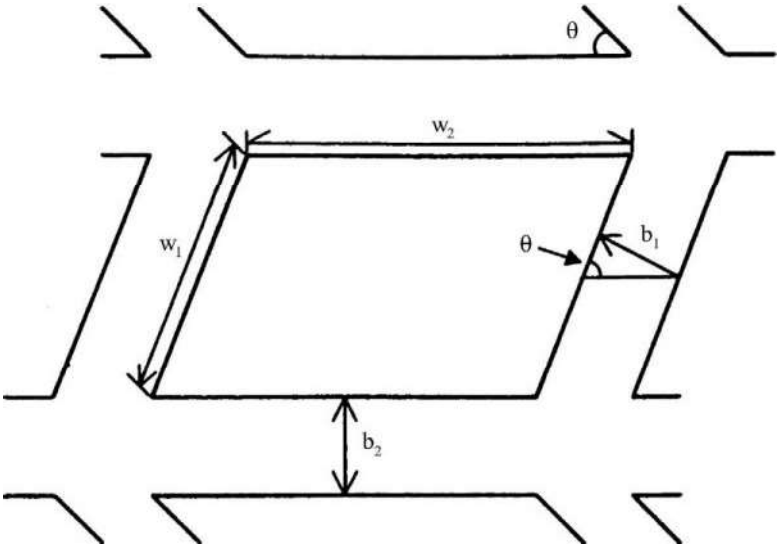

Figure 13.11 Definition of mining variables associated with a parallelepiped shaped pillar (after Galvin *et al.*, 1999).

should be the minimum width, w, for $R < 3$ and w_{eo} for $R > 6$. In the intermediate range of R, the effective width varies according to the relation

$$w_e = w\Theta_o^{(R/3-1)} = w\,\Theta \tag{13.11}$$

Equation 13.6 was then re-written as

$$S = S_o h^{\alpha} w^{\beta} \Theta^{\beta} \tag{13.12}$$

and equation 13.8 as

$$S = S_o v^a R_o^b\, \Theta^{\beta}\{(b/\varepsilon)[(R/R_o)^{\varepsilon} - 1] + 1\} \tag{13.13}$$

For the revised South African database, Galvin *et al.* (1999) found that $S_o = 6.88$ MPa, $\alpha = -0.60$ and $\beta = 0.42$. For the Australian database, $S_o = 8.60$ MPa, $\alpha = -0.84$ and $\beta = 0.51$, and for the combined South African and Australian databases, $S_o = 6.88$ MPa, $\alpha = -0.70$ and $\beta = 0.50$.

For pillar design in hard rock mines, Lunder and Pakalnis (1997) proposed a method of estimating pillar strength which integrated the results of tributary area and boundary element analysis in the so-called confinement formula. It sought to reconcile the highly empirical expressions for pillar strength with those derived from more rigorous principles based on conventional rock strength criteria, as discussed in Chapter 4, and the states of stress and confinement which develop in a pillar. It drew on a large data base of observations of pillar behaviour in Canadian mines, and also results reported by Brady (1977) for the Mount Isa Mine, Australia, Krauland and Soder (1987) for the Black Angel Mine, Greenland and Sjöberg (1992) for the Zinkgruvan Mine, Sweden.

Starting from the assumption that pillar strength S can be represented by

$$S = S(\sigma_c, \text{size}, \text{shape})$$

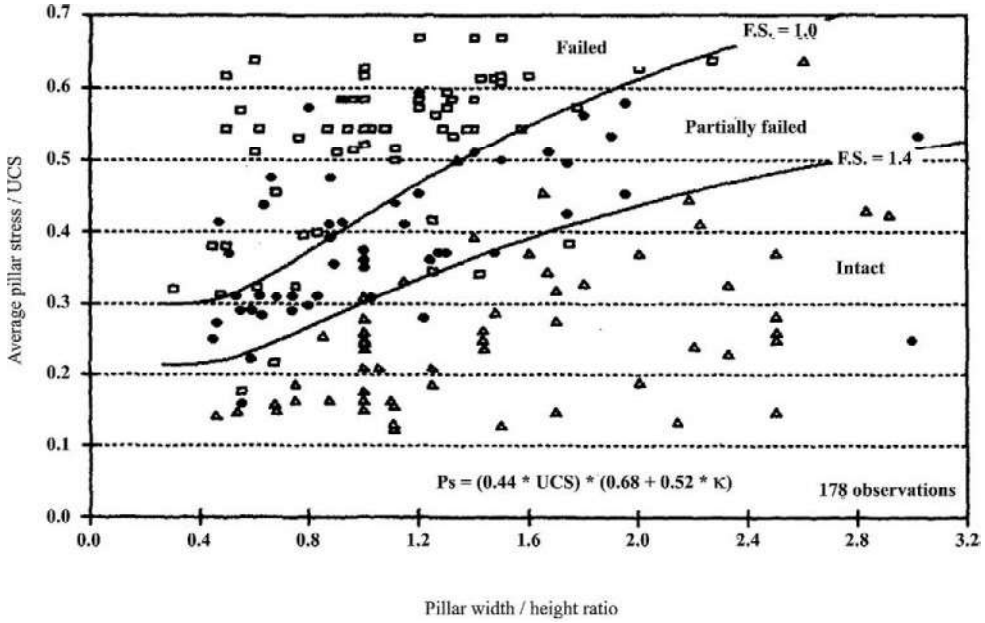

Figure 13.12 Pillar behaviour domains mapped in terms of normalized pillar stress and width/height ratio (after Lunder and Pakalnis, 1997).

it was proposed that this expression can be cast in the form

$$S = K\sigma_c(C_1 + C_2\kappa) \tag{13.14}$$

In this expression, K is a factor relating rock strength at the scale of mine pillars to rock material strength at laboratory scale, C_1 and C_2 are empirical constants and κ is a factor which represents friction mobilised in the pillar core under the conditions of confining stress which develop there.

From the data base of pillar observations, it was determined that K lies in the range of 0.30 to 0.51, from which a representative value of 0.44 was proposed.

The effect of confinement in the interior of pillars was investigated by two-dimensional boundary element analysis of various pillar shapes. It was proposed that a relation between pillar width/height aspect ratio and a term C_{pav} representing 'average pillar confinement' could be expressed by

$$C_{pav} = 0.46[\log(w/h) + 0.75] \tag{13.15}$$

The factor κ representing internal friction mobilised in pillars was derived from plots of Mohr circle diagrams of states of stress in the body of pillars. The relation proposed between the state of pillar confinement and pillar internal friction was

$$\kappa = \tan\{a\cos[(1 - C_{pav})/(1 + C_{pav})]\} \tag{13.16}$$

The large set of data on field observations of pillar performance used by Lunder and Pakalnis is recorded in Figures 13.12 and 13.13, where pillar stress (normalized in terms of the rock material strength) is plotted as a function of width/height ratio and normalized state of confinement (C_{pav}) respectively. From the field observations, it was possible to separate the modes of pillar behaviour into the domains of 'failed,'

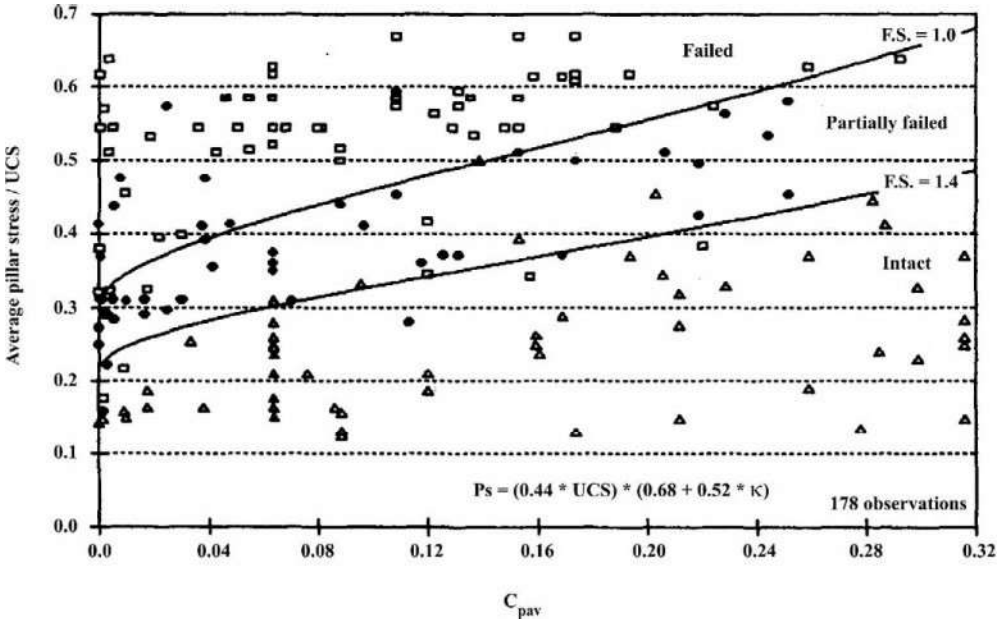

Figure 13.13 Pillar behaviour domains mapped in terms of normalized pillar stress and normalised state of internal pillar confinement, C_{pav} (after Lunder and Pakalnis, 1997).

'partially failed' and 'intact' pillars. By suitable choice of the parameters C_1 and C_2, boundaries could be constructed between the domains. With the derived values of $C_1 = 0.68$ and $C_2 = 0.52$, the resulting expression for pillar strength is

$$S = 0.44\,\sigma_c(0.68 + 0.52\,\kappa) \tag{13.17}$$

On Figures 13.12 and 13.13, the boundary lines between the 'failed' and 'partially failed' domains correspond to a factor of safety of unity. Those between the 'partially failed' and 'intact' domains correspond to a factor of safety of 1.4.

Although equation 13.17 may be used *a priori* to obtain a first estimate pillar strength, Lunder and Pakalnis (1997) advocate calibration of the expression to fit observed pillar behaviour in a particular mine setting. Given the variability of σ_c, the simplest approach is to choose a suitable value of this parameter. An alternative is to change the value of K which scales laboratory strength to the nominal field value of rock mass compressive strength, C_o.

In an alternative approach, Martin and Maybee (2000) used the Hoek-Brown brittle parameters discussed in sections 4.5.5 and 7.1 with elastic stress analyses to model the brittle pre-peak spalling of many hard rock pillars, illustrated in Figure 13.6. Following Martin (1997), they argued that this type of failure is essentially a cohesion loss process in which the frictional component of rock mass strength is not mobilised. Martin and Maybee (2000) carried out a series of numerical elastic analyses using the boundary element program Examine 2D and the Hoek-Brown brittle parameters with $m_b = 0$ and $s = 0.11$ to evaluate pillar behaviour over the range of pillar width to height ratios of 0.5 to 3. A constant value of the ratio of the *in situ* horizontal to vertical stress of 1.5 was used in the analyses. A pillar was considered to have failed when the strength to stress ratio reached 1.0 in the core of the pillar. Martin and Maybee (2000) found good agreement between their results, empirical data for Canadian mines collected by